C. R. Mecanique 338 (2010) 220–229

Contents lists available at ScienceDirect

Comptes Rendus Mecanique

www.sciencedirect.com

# FVM-BEM method based on the Green's function theory for the heat transfer problem in buried co-axial exchanger

Taoufik Mnasri [a,*], Rached Ben Younès [a], Atef Mazioud [b], Jean Felix Durastanti [b]

[a] *Department of Physics, Faculty of Sciences of Gafsa, 2112 Gafsa, Tunisia*
[b] *Laboratoire CERTES (EA 3481), IUT de Sénart, 77127 Lieusaint, France*

ARTICLE INFO

*Article history:*
Received 27 January 2010
Accepted after revision 12 April 2010
Available online 24 April 2010

*Keywords:*
Heat transfer
Forced convection
Buried exchanger
Heat transfer coefficient
Green's function

ABSTRACT

This Note presents the study of transient flow under forced convection in buried co-axial exchanger. The wall temperature as well as the wall heat flux and the heat transfer coefficient are unknown. A hybrid model consisting of a finite element method at the boundary (BEM) for the heat transfer problem on the boundary and a finite volume method (FVM) to solve the laminar flow inside solves this problem. The development of the BEM method is based on the Green's function theory. This conjugate method allows one to have fast results and to foresee the thermal behaviour of the exchanger. The heat transfer coefficients are investigated. The results are compared to those obtained using the commercial CFD package Fluent.



## 1. Introduction

The studies that relate to the non-established flow in an annular conduct subjected to a time-dependent heat flux, through the walls, are scarce [1–8]. This type of flow can be found at the inlet of the heat exchangers. The development of a complete model [2] has a major importance in the study of storage and recuperation of energy from the ground using buried vertical exchangers. The model using the Green's function theory [9] enables an entire calculation of the temperature evolution of such systems. However, it requires the use of several parameters such as the local heat transfer coefficient, which is difficult to be precisely measured and quantified. Several experimental and numerical studies were carried out [5–15], establishing correlations or empirical expressions of the convective heat transfer coefficient.

The main purpose of this Note is to determine the heat transfer coefficient of an exchanger in permanent contact with a semi-infinite medium such as the ground. The equations of energy in both parts of the system; solid and fluid, are established and coupled with the continuity relations of temperature and heat flux at the contact surface. Based on the Green's function theory, the energy equation in the semi-infinite and three-dimensional solid medium (ground volume), is transformed into an integral equation to be solved in a finite and two-dimensional medium (exchanger surface). Hence, a system of differential and integral equations governing the velocity and temperature fields is obtained. A combination between the finite volume method (FVM) and the boundary element method (BEM) allows a numerical resolution of this system. Several thermal parameters such as the temperature field and the local and average heat transfer coefficients are deduced.

The results from this established model are compared to the results obtained from a CFD code, Fluent. The CFD package Fluent is used to solve the conjugate system of equations, for the fluid and the soil, consisting of the continuity equation,

* Corresponding author.
*E-mail address:* mnassri_taoufik@yahoo.fr (T. Mnasri).

1631-0721/$ – see front matter 
doi:10.1016/j.crme.2010.04.004

**Nomenclature**

| | | | |
|---|---|---|---|
| $a_{so}$ | diffusivity of the ground | $m^2/s$ | |
| $a_f$ | diffusivity of the fluid | $m^2/s$ | |
| $D_H$ | hydraulic diameter, $D_H = 2(R_i - r_{ex})$ | m | |
| $G$ | Green's function | | |
| $\bar{G}$ | Laplace transform of Green's function | | |
| $h$ | local heat transfer coefficient at the wall | $W m^{-2}/K$ | |
| $h_\infty$ | average heat transfer coefficient at the wall (fully developed flow) | $W m^{-2}/K$ | |
| $k_f$ | thermal conductivity of the fluid | $W m^{-1}/K$ | |
| $k_s$ | thermal conductivity of the ground | $W m^{-1}/K$ | |
| $L$ | length of the exchanger | m | |
| $\vec{n}$ | the outer normal on surface $(S)$ | | |
| $P^*$ | dynamic pressure | Pa | |
| $Pr$ | Prandtl number, dimensionless | | |
| $\vec{r}$ | vector-position in the space | | |
| $\vec{r}'$ | vector-position in the space where the temperature is evaluated | | |
| $Re$ | Reynolds number, $Re = W_0 D_H \rho_f/\mu$, dimensionless | | |
| $r_{ex}$ | radius of the central tube | m | |
| $R_i$ | radius of the exchanger | m | |
| $t$ | time | s | |
| $T$ | temperature at point $\vec{r}$ and $t$ | K | |
| $T_e$ | inlet temperature of the fluid in the inner tube | K | |
| $T_m$ | mean temperature of the fluid in annular space at $z$ and $t$ | K | |
| $T_w$ | temperature of the exchanger wall at $z$ and $t$ | K | |
| $T_0$ | initial temperature field in the soil $T(\vec{r}, t=0)$ | K | |
| $u$ | radial velocity | m/s | |
| $v$ | orthoradial velocity | m/s | |
| $w$ | axial velocity in annular space | m/s | |
| $W_0$ | average velocity of fluid in the annular space | m/s | |
| $W_0'$ | average velocity of fluid in the central tube | m/s | |
| $z$ | axial coordinate | m | |

*Greek symbols*

| | | |
|---|---|---|
| $\delta$ | time step | s |
| $\Phi$ | heat flux density | $W/m^2$ |
| $\nu_f$ | cinematic viscosity of the fluid | $m^2/s$ |
| $\rho_f$ | fluid density | $kg/m^3$ |

the momentum equations (only in the fluid) and the energy equation. This package is based on the finite volume method, and requires all relevant boundary conditions to be defined. The Fluent Gambit software tool is used to generate the computational mesh. Finally, the outcomes of this in-house model are in conformity with the results given by the CFD package Fluent.

## 2. Mathematical formulation of the problem

The system is a co-axial exchanger composed of two concentric tubes inserted in the soil (Fig. 1). The interior tube made of P.V.C. is considered thermally insulator. The thermal resistance of the exterior tube is supposed to be negligible. The hot fluid enters the inner tube at temperature $T_e(t)$, circulates from top to bottom, and goes up from base in annular space at average velocity $W_0$.

### *2.1. Equation of energy propagation in the ground*

The ground is supposed homogeneous and isotropic solid medium and its thermal characteristics are considered stable and independent of the temperature. This medium of storage constitutes a domain $(D)$ surrounded by a boundary surface $(S)$ (Fig. 1). The surface $(S)$ is the union of the free surface of the soil $(St)$ and the surface of the buried exchanger $(Se)$; $(S) = (Se) \cup (St)$. The heat propagation equation in this medium is

$$\frac{1}{a_{so}} \frac{\partial T(\vec{r}, t)}{\partial t} - \Delta T(\vec{r}, t) = 0 \tag{1}$$

Its associated equation is

$$\frac{1}{a_{so}} \frac{\partial G(\vec{r}, \vec{r}', t)}{\partial t} - \Delta G(\vec{r}, \vec{r}', t) = \delta(\vec{r} - \vec{r}') \tag{2}$$

The Green's function $G(\vec{r}, \vec{r}', t)$ is the solution of Eq. (2); $G(\vec{r}, \vec{r}', t)$ is such that it is null for $t < 0$ and tends towards $\delta(\vec{r} - \vec{r}')$ at $t = 0$. If the point of observation $\vec{r}'$ is located on the surface of the exchanger $(Se)$, it is demonstrated [3] that

$$T_w(\vec{r}', t) = 2 \int_0^t \iint_{(Se)} a_{so} \left[ G(\vec{r}, \vec{r}', t-\tau) \vec{\nabla} T(\vec{r}, \tau) - T(\vec{r}, \tau) \vec{\nabla} G(\vec{r}, \vec{r}', t-\tau) \right] \vec{n} \, dS \, d\tau + 2F(\vec{r}', t) \tag{3}$$

where

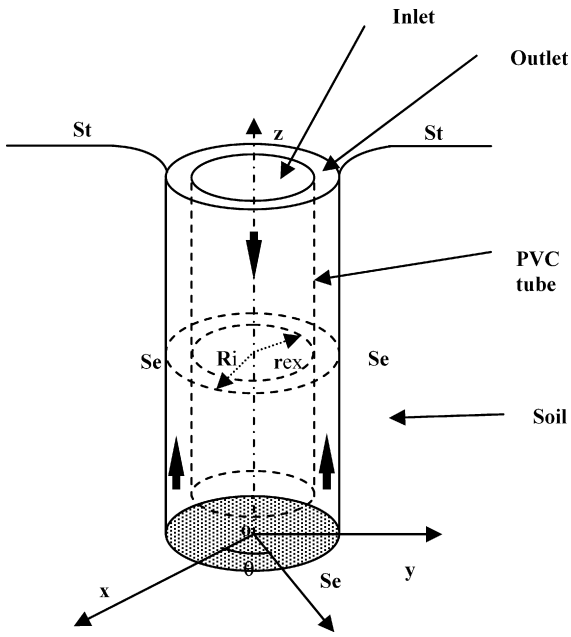


**Fig. 1.** Geometry of the exchanger.

$$F(\vec{r}',t)=\iiint_{(D)} G(\vec{r},\vec{r}',t)T_0(\vec{r})\,\mathrm{d}^3r-\int_0^t\iint_{(St)} a_{so}T(\vec{r},\tau)\vec{\nabla}G(\vec{r},\vec{r}',t-\tau)\vec{n}\,\mathrm{d}S\,\mathrm{d}\tau \tag{4}$$

*2.2. Boundary conditions at the free surface and at the exchanger surface*

The general solution of Eq. (2) is

$$G(\vec{r},\vec{r}',t)=\frac{1}{(4\pi a_{so}t)^{3/2}}\exp\left(-\frac{(\vec{r}-\vec{r}')^2}{4a_{so}t}\right) \tag{5}$$

In our study, an imposed surface temperature on $(St)$ equal to the ambient temperature $T_a(\vec{r},t)$ is considered (condition of Dirichlet)

$$T(\vec{r},t)_{z=0}=T_a(\vec{r},t) \tag{6}$$

The first term of $F(\vec{r}',t)$ which is a domain integral is eliminated in the numerical resolution by using the change of variable $T'=T-T_0$ thanks to the linearity of Eq. (1) and it does not appear explicitly. We evoke the particular case where the ambient temperature is equal to the soil initial temperature $T_0$ supposed uniform. Consequently, the second term of $F(\vec{r}',t)$ is null [3].

The contact between the ground and the exchanger is considered perfect. Consequently

$$T_w(\vec{r},t)=T_f(\vec{r},t)_{wall} \tag{7}$$

and

$$-k_f\left(\frac{\partial T_f(\vec{r},t)}{\partial n}\right)_{wall}=-k_s\left(\frac{\partial T(\vec{r},t)}{\partial n}\right)_{wall} \tag{8}$$

Using Eqs. (7) and (8), Eq. (3) becomes

$$T_w(\vec{r}',t)=2\int_0^t\iint_{(Se)} a_{so}\left[\frac{k_f}{k_s}G(\vec{r},\vec{r}',t-\tau)\vec{\nabla}T_f(\vec{r},\tau)-T_f(\vec{r},\tau)\vec{\nabla}G(\vec{r},\vec{r}',t-\tau)\right]\vec{n}\,\mathrm{d}S\,\mathrm{d}\tau \tag{9}$$

It is also mentioned that the heat flux density is expressed as follow

$$\vec{\Phi}=-k_f\vec{\nabla}T_f=-k_f\left(\frac{\partial T_f(\vec{r},t)}{\partial r}\right)_{wall}\vec{n}=h(T_m-T_w)_{wall}\vec{n} \tag{10}$$

### 2.3. Equations governing the fluid flow

The fluid density ($\rho_f$) is supposed constant. The axial symmetry of the system imposes that the flow is plane ($v = 0$) and two-dimensional ($r, z$). The equations governing the fluid flow can be written as follows:

$$\begin{cases} \dfrac{\partial u}{\partial r} + \dfrac{u}{r} + \dfrac{\partial w}{\partial z} = 0 & (11a) \\ \dfrac{\partial P}{\partial r} = 0 & (11b) \\ u\dfrac{\partial w}{\partial r} + w\dfrac{\partial w}{\partial z} + \dfrac{\partial w}{\partial t} = -\dfrac{1}{\rho_f}\dfrac{\partial P^*}{\partial z} + \upsilon_f\left[\dfrac{\partial^2 w}{\partial r^2} + \dfrac{1}{r}\dfrac{\partial w}{\partial r}\right] & (11c) \end{cases}$$

$$\frac{\partial T}{\partial t} + u\frac{\partial T}{\partial r} + w\frac{\partial T}{\partial z} = a_f\left[\frac{\partial^2 T}{\partial r^2} + \frac{1}{r}\frac{\partial T}{\partial r}\right] \quad (12)$$

In the case of turbulent flow, the model $k$–$\varepsilon$ with the wall functions of Lam and Bremhorst is used in predicting the heat transfer [16].

### 2.4. Boundary conditions and initial conditions for the whole system

No simplifying condition is imposed on the velocity or the temperature on the base level (annular space inlet). These boundary conditions are general and close to the practical. Uniform velocity and temperature are imposed at the inlet of the interior tube. Evidently, the regime is supposed established at the exit of the annular space because of the importance of the length of buried exchangers. Thus, the boundary conditions will be for the velocity field

$$\begin{cases} u\big(r = R_i^-\big) = u\big(r = r_{ex}^-\big) = u\big(r = r_{ex}^+\big) = 0 & (13a) \\ w\big(r = R_i^-\big) = w\big(r = r_{ex}^-\big) = w\big(r = r_{ex}^+\big) = 0 & (13b) \\ u(z = L) = 0 \quad \text{for } r < r_{ex} & (13c) \\ w(z = L) = W_0' \quad \text{for } r < r_{ex} & (13d) \\ \dfrac{\partial u}{\partial z}(z = L) = \dfrac{\partial v}{\partial z}(z = L) = \dfrac{\partial w}{\partial z}(z = L) = 0 \quad \text{for } r_{ex} < r < R_i & (13e) \end{cases}$$

for the temperature field:

$$\begin{cases} T_f(r, z, 0) = T_0 & (14a) \\ T_f(r, L, t) = T_e \quad \text{for } r < r_{ex} & (14b) \\ \left(\dfrac{\partial T_f}{\partial r}\right)_{r=r_{ex}^-} = \left(\dfrac{\partial T_f}{\partial r}\right)_{r=r_{ex}^+} = 0 & (14c) \\ \left(\dfrac{\partial T_f}{\partial r}\right)_{z=L} = 0 \quad \text{for } r_{ex} < r < R_i & (14d) \\ T_f(R_i, z, t) = T_w = 2\displaystyle\int_0^t\iint_{(Se)} a_{so}\left[\frac{k_f}{k_s}G(t-\tau)\vec{\nabla}T_f(\tau) - T_f(\tau)\vec{\nabla}G(t-\tau)\right]\vec{n}\,\mathrm{d}S\,\mathrm{d}\tau & (14e) \end{cases}$$

### 2.5. Calculus of the heat transfer coefficient

The mean temperature $T_m(z, t)$ is written as

$$T_m(z, t) = \frac{2}{W_0(R_i^2 - r_{ex}^2)}\int_{r_{ex}}^{R_i} T_f(r, z, t)W(r, z)r\,\mathrm{d}r \quad (15)$$

Eq. (10) enables to express the coefficient $h(z, t)$ as follows

$$h(z, t) = \frac{(k_f\frac{\partial T_f(r,z,t)}{\partial r})_{r=R_i}}{(T_w - T_m)} \quad (16)$$

## 3. Numerical model

In this Note, the discretisation scheme is an extension of that adopted by Desmons [2]. The stability of this scheme was studied by the same author. The equations governing the flow are resolved using the finite volume method (FVM) by adopting the technique of the staggered grid. The finite volume element computations are three-dimensional but thanks to the axial symmetry of the flow, a longitudinal plane of cells is used. The coupling pressure-velocity rests on the algorithm Semi-Implicit Method for Pressure Linked Revised (SIMPLER) [17], which consists in correcting the calculated velocities starting from the equations of momentum, so that these check the equation of continuity. The differential equations governing the flow are integrated over a quadrilateral computational cell $\Delta r \times \Delta z$ and on the time interval $[t, t+\delta]$. The computational grid is non-uniform and it is of $(30 \times 120)$. The grid is generated sufficiently fine near the inner and outer walls to take account of the significant variations of velocity and temperature in the boundary layer zone. An implicit diagram for the temporal discretisation is adopted. A first order upwind scheme is incorporated to represent the convective terms and stabilise the FVM method [17]. The differential equations governing the flow are integrated over a quadratic computational cell. The discretized governing equation can be written at every computational node as

$$a_P \varphi_{n,m}^{k+1} = a_W \varphi_{n,m-1}^{k+1} + a_E \varphi_{n,m+1}^{k+1} + a_S \varphi_{n-1,m}^{k+1} + a_N \varphi_{n+1,m}^{k+1} + a_0 \tag{17}$$

where all the coefficients are dependent on time and spatial steps. The indices $m, n$ and $k$ denote the coordinates $r, z$ and $t$ respectively. Thus, a nonlinear equations system is obtained where the $\varphi_{n,m}$'s at the time step $k+1$ are the only unknowns.

For the energy equation on the exchanger surface, the used method is the finite element method at the boundary (BEM) [2]. The BEM formulation is based on the fundamental solution (Eqs. (3) and (9)) of the differential equation (Eq. (1)). The BEM only requires a surface mesh. The boundary discretisation scheme consists in cutting out the exchanger wall surface in $(N)$ finite annular elements of height $\Delta$ (Fig. 1). The base represents the $(N+1)$th element, so the boundary $(Se)$ (wall and base) is subdivided into $(N+1)$ boundary elements. A sufficiently small time-step size $\delta$ is applied. $\delta$ is chosen as a submultiple of the time $t$ $(t = n\delta)$. A convolution BEM time marching scheme is developed, so it gives the solution at the time $t$. If the terms in $t$ are separated from those in $t+\delta$, the discretised equation of energy is rearranged as follow

$$\left(I + M^1\right)\vec{T}(t+\delta) - L^1\vec{\psi}(t+\delta) = \vec{P}(t,\delta) + L^0\vec{\psi}(t) - M^0\vec{T}(t) \tag{18}$$

For sufficiently weak steps of time, the thermal influence of each ring does not exceed the adjoining rings. Consequently, $G$ and $G'$ are tridiagonal matrices. Thus, the elements $G_{ii+1}, G_{i,i-1}, G'_{ii+1}$ and $G'_{ii-1}$ are taken into account in our calculation of $L_0, L_1, M_0, M_1$ and $\vec{P}(t,\delta)$.

Consequently

$$T_i(t+\delta) = \sum_{j=i-1}^{j=i+1} \left(L_{ij}^0 \psi_j(t) - M_{ij}^0 T_j(t) + L_{ij}^1 \psi_j(t+\delta) - M_{ij}^1 T_j(t+\delta)\right) + P_i(t,\delta) \tag{19}$$

with

$$\psi_i(t) = -\frac{1}{k_s}\left(k_f \frac{\partial T_i(t)}{\partial r}\right)_{r=R_i^-} \tag{20}$$

$$P_i(t,\delta) = \sum_{j=0}^{N} \int_0^t G_{ij}(t+\delta-\tau)\psi_j(\tau)\,\mathrm{d}\tau - \sum_{j=0}^{N} \int_0^t G'_{ii}(t+\delta-\tau)T_i(\tau)\,\mathrm{d}\tau \tag{21}$$

$$L_{ij}^0 = \int_0^\delta \left[1 - \frac{\tau'}{\delta}\right] G_{ij}\left(\delta - \tau'\right)\mathrm{d}\tau \tag{22a}$$

$$L_{ij}^1 = \int_0^\delta \frac{\tau'}{\delta} G_{ij}\left(\delta - \tau'\right)\mathrm{d}\tau \tag{22b}$$

$$M_{ij}^0 = \int_0^\delta \left[1 - \frac{\tau'}{\delta}\right] G'_{ij}\left(\delta - \tau'\right)\mathrm{d}\tau \tag{23a}$$

$$M_{ij}^1 = \int_0^\delta \frac{\tau'}{\delta} G'_{ij}\left(\delta - \tau'\right)\mathrm{d}\tau \tag{23b}$$

$$\psi_i(t) = -\frac{k_{f_{i,M-1}}}{k_s \Delta r_M}\left(T_{i,M}(t) - T_{i,M-1}(t)\right) \tag{24}$$

The fluid conductivity $k_f$ is supposed independent of time, so Eq. (19) takes then the following form

$$\begin{aligned} &A_{i,i-1}T_{i-1,M}(t+\delta)+(1+A_{i,i})T_{i,M}(t+\delta)+A_{i,i+1}T_{i+1,M}(t+\delta)\\ &\quad+B_{i,i-1}T_{i-1,M-1}(t+\delta)+B_{i,i}T_{i,M-1}(t+\delta)+B_{i,i+1}T_{i+1,M-1}(t+\delta)\\ &=C_{i,i-1}T_{i-1,M}(t)+C_{i,i}T_{i,M}(t)+C_{i,i+1}T_{i+1,M}(t)\\ &\quad+D_{i,i-1}T_{i-1,M-1}(t)+D_{i,i}T_{i,M-1}(t)+D_{i,i+1}T_{i+1,M-1}(t)+P_i(t,\delta) \end{aligned} \tag{25}$$

$A$, $B$, $C$ and $D$ are obviously triangular matrices. Their coefficients are

$$\begin{cases} A_{i,j}=M^1_{i,j}-B_{i,j} & (26a)\\ B_{i,j}=-L^1_{i,j}\dfrac{k_{f_{j,M-1}}}{k_s\Delta r_M} & (26b)\\ C_{i,j}=-M^0_{i,j}-D_{i,j} & (26c)\\ D_{i,j}=L^0_{i,j}\dfrac{k_{f_{j,M-1}}}{k_s\Delta r_M} & (26d) \end{cases}$$

Eq. (25) can then be written in the following form

$$\begin{aligned} &A_{i,i-1}T_{i-1,M}(t+\delta)+(1+A_{i,i})T_{i,M}(t+\delta)+A_{i,i+1}T_{i+1,M}(t+\delta)\\ &\quad+B_{i,i-1}T_{i-1,M-1}(t+\delta)+B_{i,i}T_{i,M-1}(t+\delta)+B_{i,i+1}T_{i+1,M-1}(t+\delta)=R^i \end{aligned} \tag{27}$$

where

$$\begin{aligned} R^i=&C_{i,i-1}T_{i-1,M}(t)+C_{i,i}T_{i,M}(t)+C_{i,i+1}T_{i+1,M}(t)+D_{i,i-1}T_{i-1,M-1}(t)+D_{i,i}T_{i,M-1}(t)\\ &+D_{i,i+1}T_{i+1,M-1}(t)+P_i(t,\delta) \end{aligned} \tag{28}$$

The points on the lines $i-1$ and $i+1$ are evaluated at the moment $t$, so Eq. (27) is rewritten as

$$\begin{aligned} (1+A_{i,i})T_{i,M}(t+\delta)=&R^i-B_{i,i}T_{i,M-1}(t+\delta)-A_{i,i-1}T_{i-1,M}(t+\delta)-A_{i,i+1}T_{i+1,M}(t+\delta)\\ &-B_{i,i-1}T_{i-1,M-1}(t+\delta)-B_{i,i+1}T_{i+1,M-1}(t+\delta) \end{aligned} \tag{29}$$

This equation (29) is of type

$$a_P T_{i,M}(t+\delta)=a_W T_{i,M-1}(t+\delta)+D_{n,m} \tag{30}$$

with

$$\begin{cases} a_P=(1+A_{i,i}) & (31a)\\ a_W=-B_{i,i} & (31b)\\ D_{n,m}=R^i-A_{i,i-1}T_{i-1,M}(t+\delta)-A_{i,i+1}T_{i+1,M}(t+\delta)-B_{i,i-1}T_{i-1,M-1}(t+\delta)-B_{i,i+1}T_{i+1,M-1}(t+\delta) & (31c) \end{cases}$$

To solve this nonlinear system, the Gauss–Seidel iterative method is adopted. The coupling between different regions is ensured at the boundaries using a temperature forward/flux back (TFFB) conjugate method [18,19]. This is permitted thanks to conservation of heat flux and temperature at the interface of the two different regions as formulated in Eqs. (7) and (8). The Navier–Stokes and energy equations for the internal fluid flow and the energy equation within the soil are interactively solved through a time-marching algorithm. The surface temperature obtained from the solution of fluid equations is used as the boundary condition of the boundary element method for the calculation of heat flux through the soil surface (wall). This heat flux is in turn used as a boundary condition for the fluid equations in the next time step. Transfer of nodal values from FVM and BEM (and back) independent surface meshes is performed with a compactly supported radial-basis-function interpolation [20,21].

On the contrary, of the in-house code formulated above, Fluent [22] uses a finite-volume procedure alone to solve the equations of fluid flow. Conduction heat transfer within soil is also calculated in conjugate heat transfer problems. The system is modelled in Fluent with a 3D-axisymmetric grid. A non-uniform grid is used to provide fine mesh resolution in regions where high gradients are expected. The complexity of the system geometry requires deployment of hybrid grid. Therefore, the entire computation domain is splitted into for cylindrical parts (Fig. 2). Each cylinder is a stacking of layers. The annular region is resolved by parallelepipedic structured elements. The central tube and the exterior region are resolved with prismatic unstructured meshes (Fig. 2). The model has 274 988 cells and 970 602 nodes, a number that is high enough

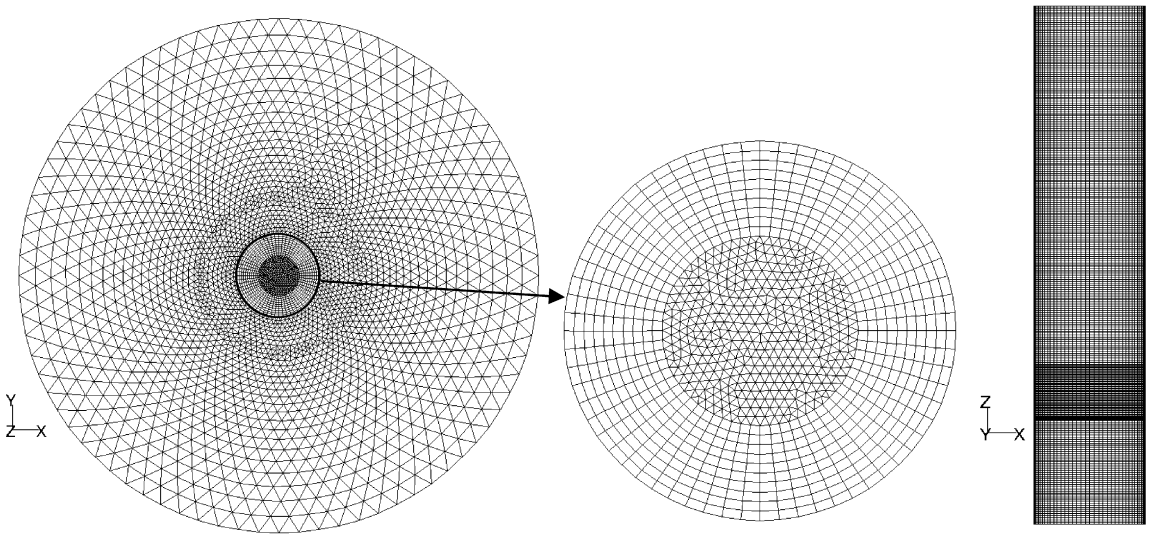


**Fig. 2.** Two views of the computational mesh.

to provide a grid-insensitive solution. The solutions are considered to converge when the normalised residual values are $10^{-6}$ for the temperature and $10^{-4}$ for the other variables.

## 4. Results and discussion

To minimise the error of truncation the use of non-uniform grid is necessary but as the mesh becomes finer, more and more steps of calculation are required, and the effect of rounding errors in the calculation would become significant. The influence of computational grid refinement on the numerical accuracy is studied. The computational grid $30 \times 120$ is found to yield the results that are independent of the number of elements used to populate the physical domain. The time step is still limited by the requirement that the truncation error must stay small, but it is found that for $1\ \text{s} \leqslant \Delta t \leqslant 40\ \text{s}$ the stability is maintained and the advancing in time is reasonable. For large time a non-uniform time interval is adopted.

The temperature field in the system is determined numerically for several combinations of Reynolds numbers $Re$ and time $t$. For $Re$ corresponding to laminar flow ($100 \leqslant Re \leqslant 2500$) and to turbulent flow ($10\,000 \leqslant Re \leqslant 30\,000$), the time envisaged is up-to one hour. The flux and the wall temperature are variable and non-uniform. They evolve in the course of time in a significant way at the beginning of the heating operation. The mode remains unsteady but it tends slowly to a permanent regime, so the mean temperature ($T_m$) and the wall temperature ($T_w$) increase with time. It can be noted that the local heat transfer coefficient is independent of the heating duration for a weak temperature variation where $\rho_f$ remains constant. It is constant and preserves the same value practically during the unsteady mode, what is confirmed by the previous correlations presented in the literature [6,7,13–15]. The axial evolution of the local heat transfer coefficient $h(z, Re)$ is given for $R_i/r_{ex} = 2$, $L/D_H = 50$, and various values of $Re$ (Fig. 3). For all $Re$, the curve $h(z, Re)$ tends asymptotically towards the value 2.95 $\text{W m}^{-2}\,\text{K}^{-1}$ (Fig. 3), which is close to the value 2.86 $\text{W m}^{-2}\,\text{K}^{-1}$ (corresponding to the Nusselt number 4.36 often quoted in most textbooks) [13,14]. The value 2.86 $\text{W m}^{-2}\,\text{K}^{-1}$ corresponds to an established flow with constant wall heat flow. Fig. 3 exhibits the code numerical predictions of the heat transfer coefficient variation along the wall line, including the Fluent numerical results. The agreement between the two numerical results is reasonable. All the relative errors are below 10% in laminar case. For the turbulent flow, all the previous correlations predict an almost linear increase in the average heat transfer coefficient with an increase in the Reynolds number. These correlations propose values, which are sometimes, differed considerably. The large discrepancies that exist among the various correlations may be due to different levels of accuracy in experimental data, especially in regard to energy balance errors [10]. The literature provides correlated expressions of the heat transfer coefficient for fully developed flow at the outer wall, which vary in $Re^{0.8}$. These correlations are valid in the case of a uniform temperature or a uniform flux imposed on the wall surface. Until now, the works witch studied the heat exchange rate of buried exchangers used these correlations [1,4,8,15,23]. The error is weak for very length exchangers, but it becomes significant in contrary case. In this work, the outer wall not subjected to any of these conditions is treated. We find that the heat transfer coefficient varies in $Re^{0.4}$ as expressed in the following equation

$$h_\infty = 0.092 Re^{0.4} \tag{32}$$

The proposed method shows good agreement with experimental correlation given by Petukhov [14] as above in Fig. 4. Therefore this last one is the most available in the case of buried exchangers. A typical temperature distribution is shown

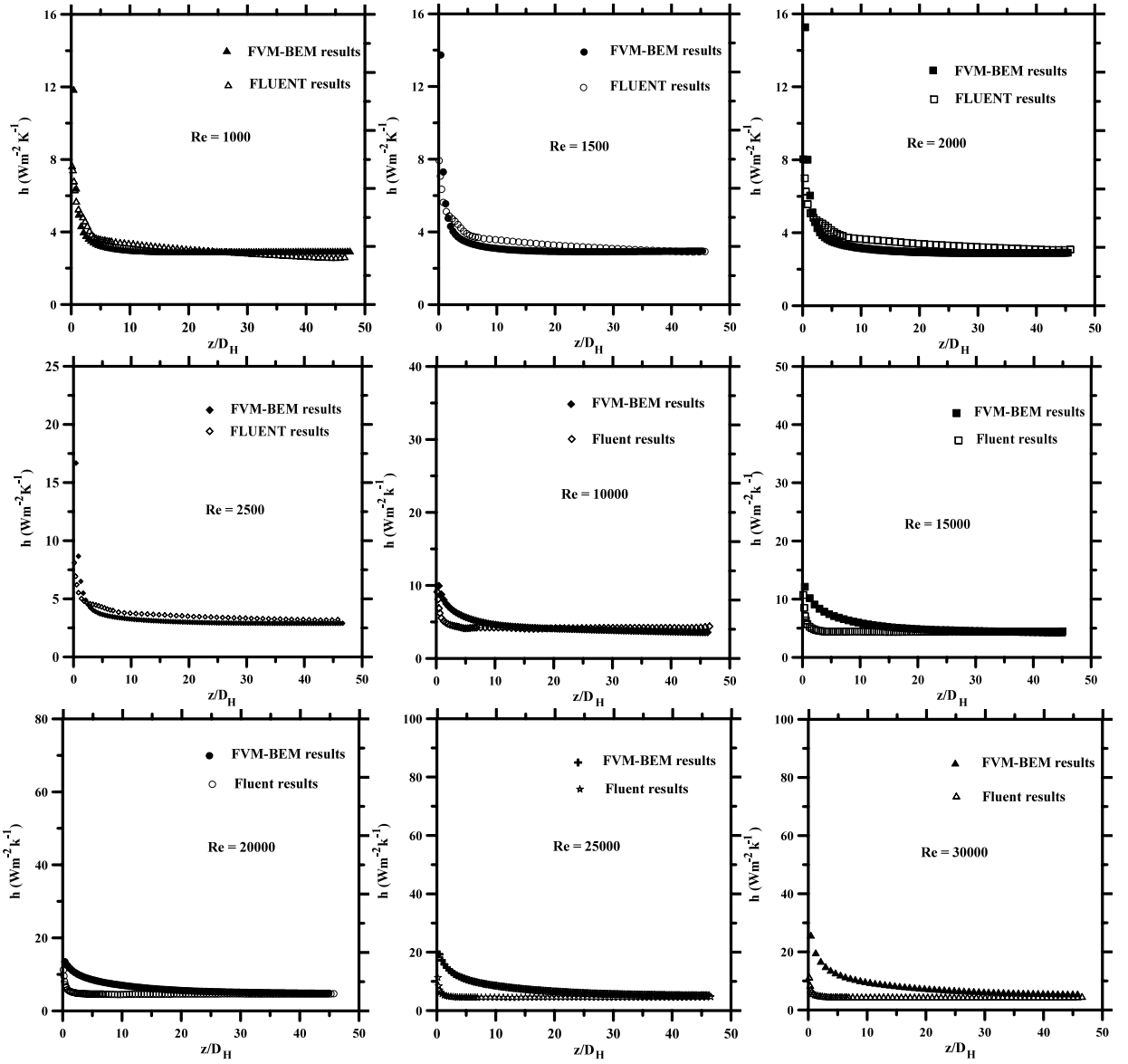


**Fig. 3.** Comparison of the predicted local heat transfer coefficient with the Fluent results at different Reynolds numbers.

in Fig. 5, for the whole domain at the Reynolds number of 20 000 and the time of 200 s. In this figure, the isotherms show the axial symmetry of the problem.

## 5. Conclusion

A combination between the finite volume method (FVM) and the boundary element method (BEM) is used to study the transient heat transfer in heat exchangers. The developed algorithm is able to manipulate a variable or constant unspecified inlet temperature in the course of time. It enables to determine certain significant thermophysical parameters such as the heat transfer coefficient, the temperature in any point of the exchanger at any moment. This study aims at the validation of the theoretical and numerical model in the case of a particular fluid (air: $Pr \approx 0.7$) and for a length to hydraulic diameter ratio ($L/D_H = 50$). It will be exploited soon to generalise the results versus various parameters such as radius ratio $R_i/r_{ex}$, length to hydraulic diameter ratio $L/D_H$, Prandtl number $Pr$, etc. It allows to have fast results and to foresee the thermal behaviour of an exchanger without doing some measures on site. What permits thereafter to reconstitute the response of an exchangers association used in the case of the air-conditioning of a greenhouse or a dwelling. The theoretical model as well as the simulation method can be useful to identify the boundary conditions like the heat flux or the convection coefficient, in industrial processes confronted with this kind of systems.

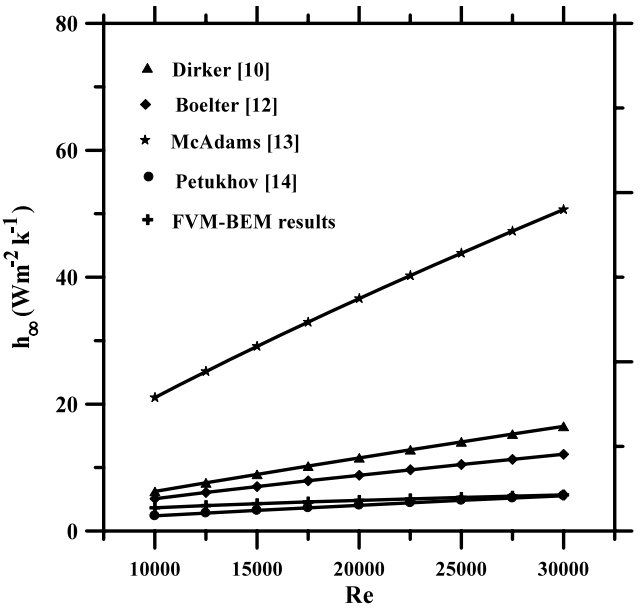


**Fig. 4.** Comparison between heat transfer coefficients in fully developed flow versus Reynolds numbers.

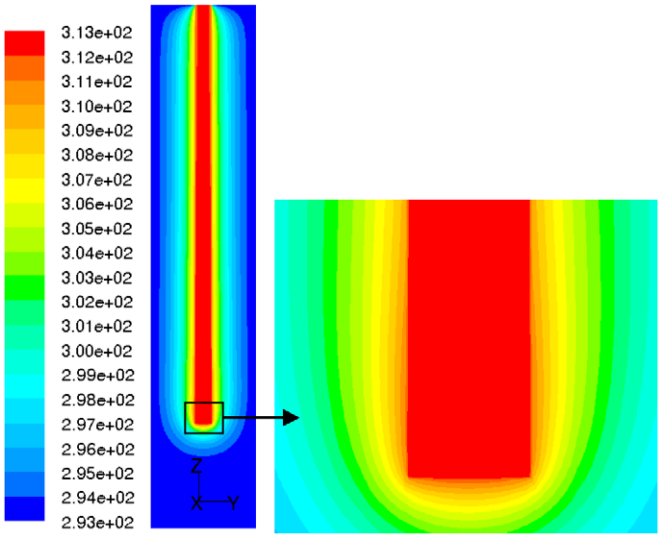


**Fig. 5.** Contours of temperature at $Re = 20\,000$ and $t = 200$ s.

## Acknowledgements

The authors thank Prof. R. Schiestel of Institut de Recherche sur les Phénomènes Hors Equilibre (I.R.P.H.E), UMR 6594 CNRS, Marseille (France) for his generous helps.

## References

[1] V.-C. Mei, S.-K. Fischer, A theoretical and experimental analysis of vertical, concentric-tube ground-coupled heat exchangers, Oak Ridge National Laboratory, Martin Marieta Energy Systems, Inc., 1984.
[2] J.-Y. Desmons, Formulation et résolution numérique de problèmes aux limites appliquées aux générateurs de chaleurs tubulaires enterrées, Thèse de Doctorat d'Etat, Université de Valenciennes, 1984.
[3] J.-Y. Desmons, R. Ben Younès, Prévision à long terme de la réponse d'un stockage de chaleur sensible dans le sol, Int. J. Heat Mass Transfer 40 (1997) 3119–3134.
[4] J.-W. Stevens, Coupled conduction and intermittent convective heat transfer from a buried pipe, Heat Transfer Engrg. 23 (2002) 34–43.
[5] S.-V. Mokamati, R.C. Prasad, Transient-based technique for the evaluation of the overall heat transfer coefficient in a concentric tube heat exchanger, Int. J. Heat Exchangers 5 (2004) 15–28.

[6] T. Mnasri, R. Ben Younès, M. Raddaoui, S. Elouragini, Simulation of convective heat-transfer coefficient in a buried exchanger, Amer. J. Appl. Sci. 5 (2007) 927–933.
[7] T. Mnasri, R. Ben Younès, A. Mazioud, J.F. Durastanti, Étude du coefficient de transfert d'un échangeur bi-tubulaire enterré en régime instationnaire, in: Congrès français de thermique (SFT), Ile des Embiez, vol. 1, 2007, pp. 361–366.
[8] P. Hollmuller, Utilisation des échangeurs air/sol pour le chauffage et le rafraîchissement des bâtiments. Mesures in situ, modélisation analytique, simulation numérique et analyse systémique, Ph.D. thesis, Université de Genève, 2002.
[9] H.-S. Carslaw, J.-C. Jager, Conduction of Heat in Solids, Oxford University Press, London, 1959.
[10] J. Dirker, J. Meyer, Convective heat transfer coefficients in concentric annuli, Heat Transfer Engrg. 26 (2005) 38–44.
[11] A. Quarmby, Some measurements of turbulent heat transfer in the thermal entrance region of concentric annuli, Int. J. Heat Mass Transfer 10 (1967) 267–276.
[12] M.K.L. Boelter, G. Young, H.W. Inversen, Distribution of heat transfer rate in the entrance section of circular tube, National Advisory Committee for Aeronautics, Technical Note 1451, 1948.
[13] W.H. Mac Adams, Transmission de la chaleur, McGraw-Hill, New York, 1954.
[14] J.-H. Lienhard IV, J.-H. Lienhard V, A Heat Transfer Textbook, 3rd edition, Phlogistron Press, Cambridge, 2002.
[15] M. Dalle Donne, E. Meerwald, Heat transfer and friction coefficients for turbulent flow of air in smooth annuli at high temperatures, Int. J. Heat Mass Transfer 16 (1973) 787–809.
[16] C.-K.-G. Lam, K. Bremhorst, A modified form of the $k$–$\varepsilon$ model for predicting wall turbulence, J. Fluids Engrg. 103 (1981) 456–460.
[17] S.-V. Patankar, Numerical Heat Transfer and Fluid Flow, Series in Computational Methods in Mechanics and Thermal Sciences, McGraw-Hill, New York, 1980.
[18] E. Divo, E. Steinthorsson, F. Rodriguez, A.-J. Kassab, J.-S. Kapat, Glenn-HT/BEM conjugate heat transfer solver for large-scale turbomachinery models, NASA Glenn Research Center, NASA CR-2003-212195, 2003.
[19] A. Kassab, E. Divo, J. Heidmann, E. Steinthorsson, F. Rodriguez, BEM/FVM conjugate heat transfer analysis of a three-dimensional film cooled turbine blade, Int. J. Numer. Methods Heat Fluid Flow 13 (2003) 581–610.
[20] J.-G. Wang, G.-R. Liu, A point interpolation meshless method based on radial basis functions, Int. J. Numer. Methods Engrg. 54 (2002) 1623–1648.
[21] G.-B. Wright, B. Fornberg, Scattered node compact finite difference-type formulas generated from radial basis functions, J. Comput. Phys. 212 (2006) 99–123.
[22] Gambit User Manual, ver. 6.2, Fluent, Inc., 2005.
[23] P. Tittelein, G. Achard, E. Wurtz, Modelling earth-to-air heat exchanger behaviour with the convolutive response factors method, Appl. Energy 86 (2009) 1683–1691.